Chalcogenide Letters Vol. 21, No. 7, July 2024, p. 513 - 527

Synthesis and physical characterization of novel Ag_2S-CdS /Ag /GNP ternary nanocomposite

L. R. Gahramanli[a,b,*], S. Bellucci[a], M. B. Muradov[b], M. La Pietra[a], G. M. Eyvazova[b], C. V. Gomez[a], J. Bachmann[c]
[a]*NEXT laboratory, INFN, LNF, Via E. Fermi 54, Frascati, Roma, Italy*
[b]*Nano Research Laboratory, Baku State University, Academic Zahid Khalilov Street 23, Baku, Azerbaijan*
[c]*Department of Chemistry and Pharmacy, Institute of Chair 'Chemistry of Thin Film Materials', Friedrich- Alexander-Universität Erlangen-Nürnberg (FAU), 91058 Erlangen, Germany*

A new type of Ag_2S-CdS/Ag/GNP nanocomposite material was successfully synthesized in the presented work. The structural and physical properties of compounds were studied separately and together. Ag_2S-CdS/Ag/GNP nanocomposite materials were studied by X-ray diffraction (XRD), Ultraviolet-Visible (UV-Vis), Fourier Transform Infrared (FTIR), Raman spectroscopy and Scanning Electron Microscopy (SEM). Based on the results, Ag nanowires (NWs) were successfully synthesized, and then it was determined that during the hybridization process, two phases of acanthite Ag_2S and the cubic crystal system of Ag_2O were formed. Then, Ag_2S-CdS NWs were formed from mixed monoclinic Ag_2S and hexagonal CdS. In the absorption spectrum of Ag NWs, the main absorbance peaks were observed at 357.3 nm and 380.2 nm. The energy gap (E_g) values of the Ag sample are 3.8 eV. The band gap value of Ag_2S (2.5, 3.8, 4.6 eV) and Ag_2S-CdS (2.5, 3.8, 4.8 eV) have a triple value due to the formation of a hybrid structure. The Raman spectrum of Ag_2S-CdS belongs to longitudinal-optical (LO) phonon modes of zinc-blende phase CdS and for the 1, 2, and 3 times spin-coated samples on the surface of GNP/PVA have observed all characteristic Raman peaks, which belong to NWs at 485.13 cm^{-1}, and 960.22 cm^{-1}.

(Received May 5, 2024; Accepted July 8, 2024)

Keywords: Silver NWs, GNP, Physical properties, Raman spectra

1. Introduction

Silver-based nanomaterials have gained great attention in recent years due to their wide range of application fields, especially, 1D structured materials with high aspect ratios among them. Their unique optical, electrical, and thermal properties are superior to those of their bulk materials [1]. Ag NWs, which belong to 1D materials, are distinguished by their high conductivity property. Due to its bandgap energy of approximately 3.84 to 3.89 eV [2], the n-type Ag_2S semiconductor can form a heterojunction with CdS, achieving enhanced charge carrier separation and harvesting a broader absorption spectrum.

The need to use carbon-based materials, which are also economically favorable, as an alternative material to solar cells, is one of the current issues. At the same time, from the point of view of chemical stability, it is more appropriate to use these materials as solar cells. In the literature, there are several research works on the use of carbon-based materials to obtain high efficiency [3-5]. The mentioned research works are very new in the literature. To have high efficiency in solar cells, high efficiency cannot be achieved due to environmental contamination of solar panels [6]. In this regard, the use of Ag_2S NWs in the form of heterostructures to obtain clean surfaces and, at the same time, the synthesis of GNP-based Ag_2S-CdS/Ag/GNP composite materials (by bulk heterojunction) method (BHJ) and a detailed study of their physical characteristics are considered interesting issues. It is planned to prepare n-type Ag_2S-CdS, then Ag NWs (p-type), and finally a

* Corresponding author: gahraman.lala@gmail.com
https://doi.org/10.15251/CL.2024.217.513

layer of transparent and flexible GNP with high electrical conductivity. Ag_2S has excellent electronic and photo-conductive properties. Ag_2S can extend the solar absorption spectrum of CdS. NWs's directional charge transport properties enable increased solar cell efficiencies. Ag NWs have extraordinary superiority in electrical conductivity, low surface strength, and high transparency. The last-generation material in PV - GNP's properties make it useful in heterojunction solar cells. The BHJ concept's adaptation is one of the most efficient strategies to reduce carrier travel between NWs. The carrier's diffusion distance to the donor and acceptor interface phases is shortened according to the BHJ concept's key tenet. A self-segregated three-dimensional (3D) network on the nanoscale is then produced by each NW system.

2. Experimental part

2.1. Materials and characterization

Ethylene glycol (EG) (anhydrous, 99.8%), polyvinylpyrrolidone (PVP), sodium chloride (NaCl) (99.0%), potassium bromide (KBr), copper (II) chloride dihydrate (99.9%), silver nitrate ($AgNO_3$) (≥99.0%), Na_2S(≥99.9%), $Cd(CH_3COO)_2{\cdot}2H_2O$ (98%), graphite (<20 μm, synthetic), and isopropyl alcohol (70% reagent) were purchased Sigma Aldrich.

To determine the structural properties of these materials using Mini-flex 600 (Rigaku XRD), as an Ultraviolet-Visible spectrophotometer Specord 250, and for transmittance spectra of FTIR spectroscopy Agilent (Agilent Cary 630 FTIR Spectrometer). To get the Raman spectrum, an InVia microscope (Renishaw, Wotton-under-Edge, UK) was employed. SEM (Jeol JSM-F100 with EDX), trinocular Motic BA310 cameras were used for characterization.

2.2. Fabrication of Ag NWs

With some modifications, silver NWs are synthesized using the polyol method described in the literature [7, 8]. EG is used as a solvent as well as a silver-reducing agent. As a capping agent, PVP with a molecular weight of 360,000 is used. Salts such as NaCl and KBr are used to balance charges and aid in nucleation and growth. For the synthesis of Ag NWs, 5 ML EG solution, which is initially used as a reducing agent for the synthesis of Ag NWs, is stirred at a temperature of 155°C for 1 hour. 1.5 ml 0.147 M PVP is dissolved in EG for 2 hours at an elevated temperature before cooling to room temperature. In addition, NaCl and KBr are dissolved in EG. To remove oxygen, the PVP solution is bubbled with nitrogen gas for 2 hours. Meanwhile, 1.5 ml 0.094 M $AgNO_3$ dissolves in EG. PVP solution is placed in an oil bath and the temperature is raised to 160°C in a nitrogen atmosphere. At this temperature, the stocked NaCl and KBr solutions are injected into the PVP solution. After 10 minutes of mixing, the prepared $AgNO_3$ solution is injected into the reaction solution drop by drop. The reaction is continued for another hour after the injection of $AgNO_3$.

The reaction solution is cooled to room temperature. To precipitate Ag NWs, acetone is poured into the reaction solution. After 5 minutes of centrifugation, the precipitates are collected and dispersed in ethanol. To remove unnecessary chemicals, this washing process is repeated twice. Then, the final products are dispersed in ethanol.

2.3. Fabrication of Ag-Ag_2S NWs

The second step involves the formation of Ag-Ag_2S NWs. This is typically done through a controlled sulfidation process where Ag NWs react with a sulfur source to form Ag_2S on their surfaces. To synthesize Ag-Ag_2S NWs, firstly prepared 1.5 mL of Ag NWs in ethanol. Then, the solution of Ag NWs is poured with 1.5 ml of Na_2S in distilled water as a sulfur source and mixed by handshaking at room temperature for 5 minutes. For the reaction, 0.001M concentrated Na_2S is used. Then, the solution is precipitated with acetone, and the final Ag-Ag_2S is collected and dispersed in ethanol after centrifugation.

2.4. Fabrication of Ag-Ag_2S-CdS nanocomposites

In the next step to obtaining Ag-Ag_2S-CdS NWs, 0.2 M concentrated $Cd(CH_3COO)_2{\cdot}2H_2O$ solution is added to the formation of Ag-Ag_2S-CdS nanocomposite and mechanically stirred at room temperature for 5 minutes. This step aims to introduce Cd ions to form CdS on the surface of the

Ag-Ag_2S NWs. To remove unreacted residue elements, the final solution was centrifuged twice, and dispersed in an ethanol solution.

2.5. Fabrication of GNP

The synthesis process of GNP was carried out by exfoliating of the graphite at the NEXT laboratory of INFN, LNF (Frascati, Rome, Italy) [9, 10]. After obtaining graphene, it is necessary to evaporate isopropyl alcohol, which used a synthesis process. It was oven-dried at 80°C for a date. Finally, pure GNP was obtained for further processing.

2.6. Preparation of samples for analysis

For appropriate analysis, Ag_2S-CdS /Ag NWs are deposited on the surface of GNP, or Ag_2S-CdS/Ag NWs/GNP are deposited on the surface of the glass.

3. Result and discussion

3.1. XRD analysis

To determine the crystalline structure of the samples, XRD analysis was employed. The XRD patterns of Ag NWs (Fig.1.a), Ag_2S-CdS (Fig.1.b), and GNP (Fig.1.c) are shown in Fig. 1.

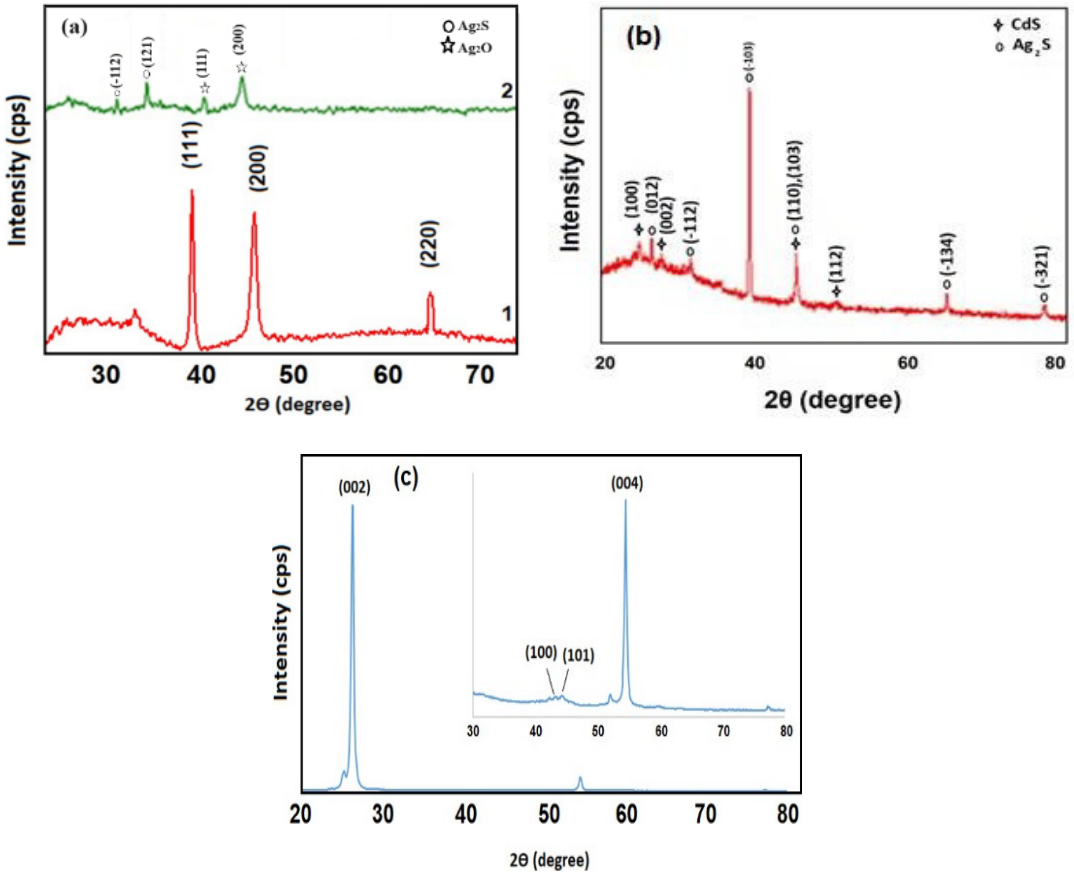

Fig. 1. XRD pattern of a) Ag NWs; b) Ag_2S-CdS and c) GNP.

Pure Ag NWs are formed, as seen in the XRD pattern (Fig.1.a.1). The diffraction pattern shows three main peaks at 2θ=38.0°, 44.8°, and 63.7°. These peaks correspond to the ICDD 00-001-1167 card number [11], and they are indexed by the (111), (200), and (220) Miller indices,

respectively. These peaks indicate that the crystallite size is d=2.36, 2.01, and 1.45 nm. After hybridization (Fig.1.a.2), the XRD pattern shows that Ag_2S and Ag_2O were formed and matched acanthite Ag_2S (JCPDS Card no.14-0072) and the cubic crystal system of Ag_2O (JCPDS Card no. 89-3722).

Fig.1.b shows the XRD pattern of Ag_2S-CdS. According to the XRD results, the peaks are observed in the diffraction pattern at 2θ=23.5°, 25.2°, 26.8°, 31.7°, 38.1°,44.3°, 51.3, 64.4° and 77.4° [12]. According to the obtained results, it is possible to see that the obtained structure corresponds to the mixed phase. So, 2θ=23.5°, 26.8°, 44.3°, and 51.3° correspond to the hexagonal (wurtzite) crystallite phase of CdS with card number JCPDS No. 75-1545 41-1049 and are labeled as (100), (002), (110), and (112), respectively [13].

The 2θ=25.2°, 31.7, 38.1°, 44.3°, 64.4° and 77.4° peaks observed in the XRD pattern correspond to monoclinic Ag_2S and are labeled (012), (-112), (-103), (103), (-134), and (- 321), respectively [14,15]. Among these peaks, the 2θ=44.3° peak coincides with both phases and shows itself as the most intense peak after the most intense peak belonging to Ag_2S.

The XRD pattern of GNP is shown in Fig.1.c. The peak observed at 2θ =26.4° corresponds to (002) with an inter-spacing of 3.35, and the peaks observed at 2θ =43.5° and 2θ =44.6° correspond to (100) and (101) correspond to Miller indices [16]. Since the intensity of the (002) peak is large, other peaks are weakly observed against its background [17]. The peak observed at 2θ =54.5° corresponds to the (004) crystalline plane. The mentioned peaks are characteristic peaks belonging to graphene nanoplatelets.

3.2. UV-Vis spectroscopy

The results obtained from the sample analysis by UV-Vis spectroscopy are given in Fig.2.

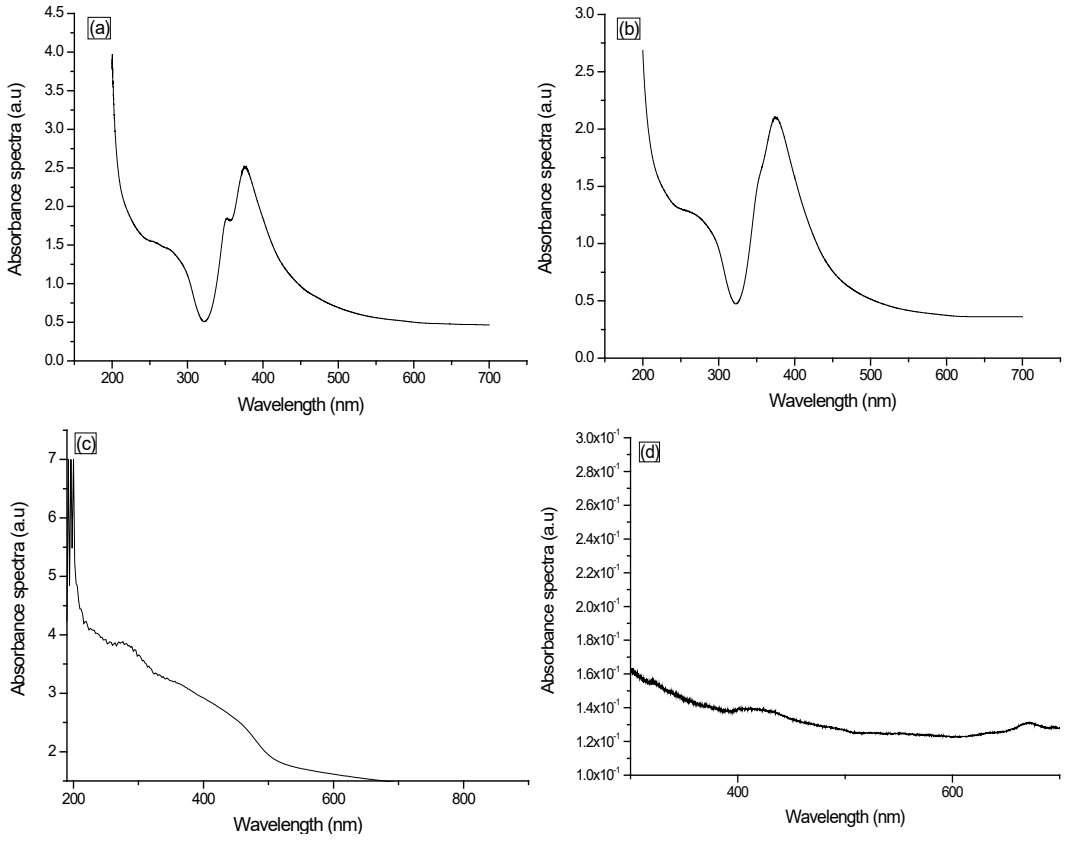

Fig. 2. Absorbance spectra of (a) Ag NWs; (b) Ag_2S NWs; (c) Ag_2S-CdS and (d) GNP.

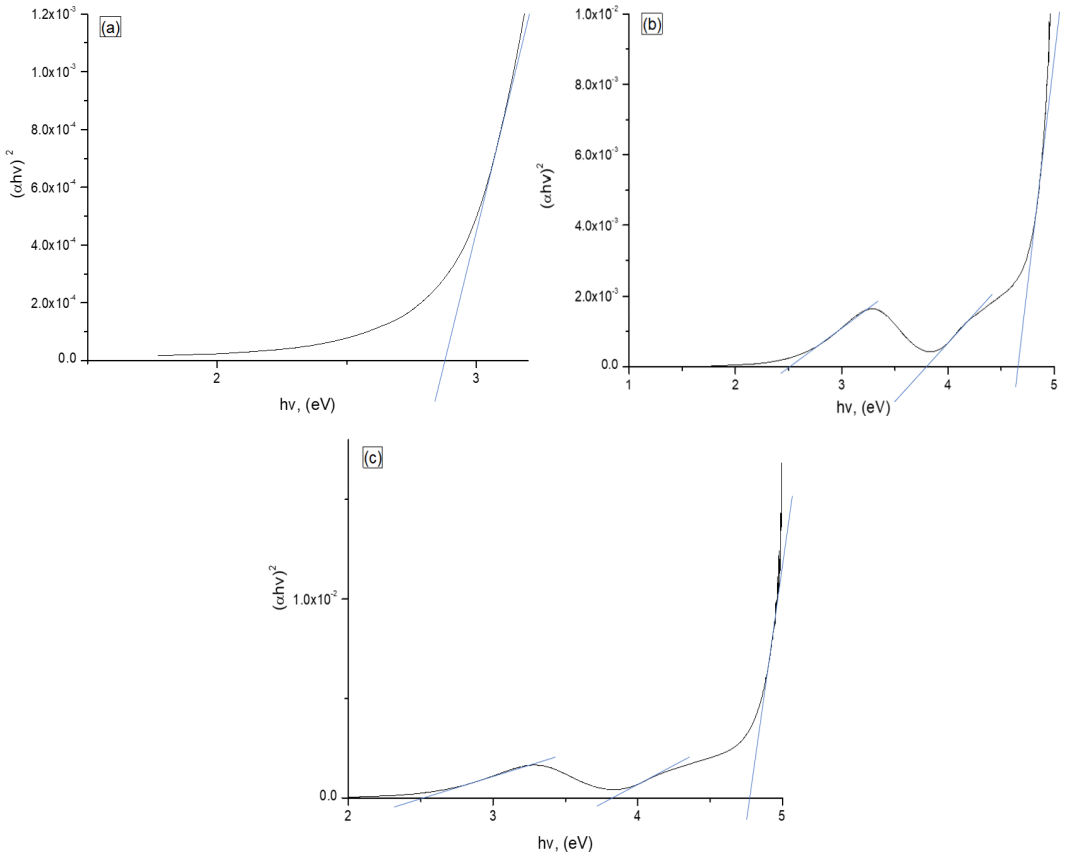

Fig. 3. Determination of band gap value of a)Ag NWs; b)Ag_2S NWs and c)Ag_2S-CdS by Tauch relation.

Fig. 2.a shows the absorbance spectra of Ag NWs, Ag_2S NWs (Fig.2.b), Ag_2S-CdS (Fig.2.c), and GNP (Fig.2.d). Ag NWs exhibit strong plasmonic behavior due to their high electrical conductivity and unique geometry. Also, plasmonic resonance frequency depends on free-carrier concentration, which is proportional to the square root of free-carrier concentration [18]. The dimensions and aspect ratios of the NWs can influence the specific plasmonic resonances observed in the optical spectrum. Here, two characteristic absorbance peaks of AgNWs were observed, and both of them were related to surface plasmon resonance for each type of silver structure [19]. It is considered that the peak at 357.3 nm corresponds to a shorter wavelength, indicating a higher energy resonance. The peak at 380.2 nm corresponds to a longer wavelength, indicating a lower energy resonance. Peaks that are observed maximum and minimum wavelengths are related to the transverse plasmon resonance, and the quadrupole resonance, respectively [20].

As a result of the sulphidization process, the position and width of the peaks change as the mixture reacts—the transverse plasmonic resonance peak shifts to the right, or red-shifts. The formation of Ag_2S crystals on the surface of Ag NWs is attributed to this phenomenon. Ag_2S nanostructures on Ag NWs grow larger and thicker as hybridization progresses. As the reaction progresses, the surface of Ag NWs becomes increasingly surrounded by Ag_2S. As hybridization progresses, the UV-Vis absorbance peaks are red-shifted.

To create hybrid structures, coverage of the Ag_2S surface with CdS was carried out. The absorbance spectra of the Ag_2S-CdS nanocomposite are demonstrated in Fig.2.c It is determined that the peak observed approximately at the 300 nm absorbance range is related to the intrinsic band gap absorption of CdS [21]. So, it was once confirmed that Ag_2S-CdS nanostructures were created.

The absorbance spectrum of GNP is similar to the research work [22]. From the literature, the weak absorbance peaks in the 320-680 nm range are characteristic of GNP (Fig.2.d).

Fig. 3 shows the band gap values of Ag NWs (Fig.3.a), Ag_2S NWs (Fig.3.b) and Ag_2S -CdS (Fig.3.c) determined by Tauch plots. Based on the calculation, the band gap value of pure Ag NWs

is 3.8 eV (Fig.3.a). In the different diameter numbers (d=42-104 nm), the E_g value is changed from 2.11 eV to 2.37 eV [23]. From SEM images (Fig.11.a), it is determined that the diameters of pure Ag NWs are about ~0.2-0.3 µm. In the literature, it is mentioned that with increasing diameter of Ag NWs, the band gap values are increased. So, by considering the band gap value according to the maximum diameter, the band gap value of synthesized Ag NWs is increased by increasing the diameter of Ag NWs.

As a result of hybridization, triple band gap values were obtained from the determination of the band gap energies of Ag_2S NWs by the Tauch relation method. Thus, the band gap value was 2.5, 3.8 and 4.6 eV. From this, it can be seen that during the hybridization in the composite material, in addition to Ag_2S, Ag_2O was formed. From the mentioned values, it was determined that the E_g value of Ag_2S is 2.5 eV, the E_g value of Ag NWs is 3.8 eV, and the E_g value of Ag_2O is equal to 4.6 eV. This result is also confirmed by XRD results.

In the next stage, at the stage of obtaining Ag_2S-CdS nanostructures, the band gap value again received a triple value and these values received the values of 2.5, 3.8, and 4.8 eV. These values are listed in the order of Ag_2S, Ag, and CdS.

Since, the absorbance spectra of the samples consisting of 1, 2, and 3 layers deposited on the GNP are identical to the absorbance spectrum of the GNP, it was not possible to obtain any information.

3.3. FTIR analysis

To determine the possible interaction between the elements was carried out FTIR analysis. FTIR analysis of Ag and Ag_2S-CdS nanostructures deposited on a glass substrate is given in Fig.4.a. Since glass is used as a substrate the spectrum of pure glass is also added.

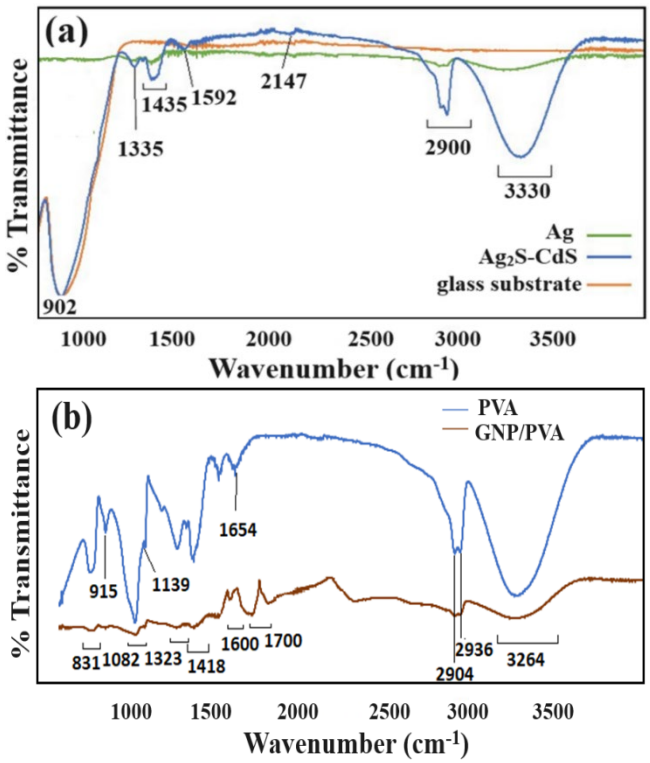

Fig. 4. FTIR spectrum of a) Ag and Ag_2S-CdS; b) GNP/PVA.

In the 2900 cm^{-1} range, a sharp peak was observed for pure Ag (2911 cm^{-1} and 2939 cm^{-1}) and a relatively weakly observed for Ag_2S-CdS (2899 cm^{-1} and 2966 cm^{-1}) scissor-shaped crossed peak is due to the vibration of CH_2 groups of PVP used during the formation of Ag NP [24]. The

formation of scissor-shaped peaks in the FTIR spectrum is most commonly observed when analyzing molecules or functional groups with coupled oscillators. Coupled oscillators are molecular vibrations that involve multiple bonds or groups that interact with each other. In these cases, the energies of the vibrational modes are no longer independent but become coupled, resulting in changes in their frequencies and intensities. For this reason, during the formation of pure Ag NWs, the CH_2 bond corresponding to the mentioned wavenumber formed a scissor-shaped peak with a relatively small intensity due to its weak interaction only with Ag, and in the FTIR spectrum of other Ag_2S-CdS nanocomposite material, this functional group is associated with Ag_2S NWs as well as CdS creates mutual communication with and manifests itself sharply.

Compared with the literature, it was concluded that the peaks observed at 1435 cm^{-1} wavenumber for Ag and Ag_2S are related to the C-H bending vibration of PVP in Ag NWs. However, the peak related to Ag_2S-CdS is more clearly observed than the peak related to Ag in the mentioned wavenumber. Because the E_g of Ag_2S-CdS is greater than pure Ag, materials with higher E_g values have higher intensities in the infrared region (because they absorb less in this region).

The peak observed at 3330 cm^{-1} wavenumber is related to O-H stretching [24]. This absorption is observed for both Ag and Ag_2S-CdS. The only difference is in the absorption intensity. This is because Ag NWs have characteristic absorption peaks and intensities with PVP. However, since Ag_2S-CdS nanostructures have a more complex structure compared to pure Ag, the existence of Ag-S and Ag-Cd and Cd-S bonds here, beyond the characteristic absorption spectrum, observes more absorption. At the same time, the diameter of NWs can affect the absorption spectrum. Thus, while Ag NWs have a uniform 1D structure, Ag_2S-CdS nanostructures are formed on a pure 1D structure, and it is clear that its diameter is larger than the diameter of pure Ag NWs. Therefore, significant differences are observed in the absorption intensities of Ag and Ag_2S-CdS in different parts of the FTIR spectrum.

A weak peak observed at 2147 cm^{-1} is attributed to the Ag-S bond, which confirms the formation of Ag_2S [25].

The absorption peak corresponding to 1335 cm^{-1} is related to O-C=O asymmetric stretching vibration [26]. A weak intensity peak at 1592 cm^{-1} is related to the bending vibration of C=N [27]. Absorption peaks belonging to Ag and Ag_2S-CdS nanostructures separately prove the presence of chemical bonds between the elements of the composite materials.

Fig 4.b. shows the FTIR spectrum of pure PVA and GNP/PVA composite materials. The absorption observed at 3264 cm^{-1} wavenumber is due to the O-H stretching of PVA. Absorptions of 2936 cm^{-1} and 2904 cm^{-1} are attributed to asymmetric stretching of CH_2 and symmetric stretching of CH_2, respectively. 1654 cm^{-1} (due to water absorption), 1418 cm^{-1} (CH_2 bending) 1323 cm^{-1} (δ (OH), rocking with CH wagging), 1139 cm^{-1} (shoulder stretching of C-O) (crystalline sequence of PVA), 1082 cm^{-1} (stretching of C-O and bending of OH) (amorphous sequence of PVA), 915 cm^{-1} (CH_2 rocking), 831 cm^{-1} (C-C stretching) is observed in the spectrum [28]. The –C–OH stretching observed in the FTIR spectrum indicates the formation of connections between PVA and GNP, that is, the bonding of the hydroxyl group of PVA and the carbonyl groups of GNP [29].

The absorption observed in the range of 1600 cm^{-1} is characteristic of GNP. The presence of sp^2 hybridized carbon atoms in the graphene structure leads to characteristic peaks in the range of 1500-1600 cm^{-1}. This region corresponds to the stretching vibrations of the carbon-carbon (C=C) bond [30].

The peak observed in the interval of 1700 cm^{-1} involving carbonyl groups (C=O), a peak can be observed around 1700-1750 cm^{-1}, representing the stretching vibrations of these groups [31]. The decrease in the intensity of the peak related to PVA is due to the formation of GNP at the nodes of the chemical bonds present here.

Other samples were obtained by depositing 1, 2, and 3 times Ag and Ag_2S-CdS on the GNP/PVA composite by spin coating, respectively. The FTIR spectrum of 1, 2, and 3 deposited layers are shown in Fig.5.

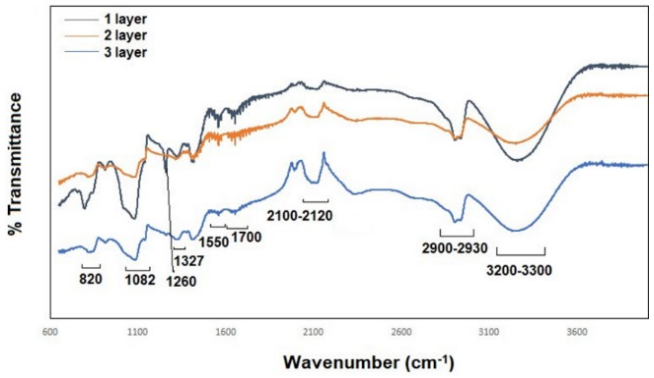

Fig. 5. 1, 2, and 3 times deposited layers on GNP/PVA composite.

The peak observed at 3200-3300 cm^{-1} wavenumber belongs to the PVA stretching of O–H bonds [32]. The decrease in the intensity of this peak with the increase in the number of deposited layers is attributed to the fact that these layers cover the surface of the GNP/PVA composite. As a result, the intensity of the characteristic peak related to PVA is also reduced.

The peaks at 2900-2930 cm^{-1} regions are due to both the characteristic absorption at 2900 cm^{-1} of GNP and the methylene groups' C–H stretching of PVA at 2930 cm^{-1}. In the scientific literature [32], when comparing pure PVA and GNP/PVA composite, it was observed that a new scissor peak was formed at 2890 cm^{-1} when GNP was deposited on PVA. This is the evidence of chemical bonding between PVA and GNP.

The absorption observed in the range of 2100-2120 cm^{-1} observed for all three samples is related to the Ag-S bond [21]. The sharp peak observation of the absorption of this peak with the increase in the number of deposited layers is evidence of the strengthening of the chemical bond depending on the number of layers, and the formation of stronger bonds.

Peak stretching vibrations from C = O carbonyl stretch were observed at 1700 cm^{-1}, absorption observed at 1550 cm^{-1} C = C stretching vibrations of aromatic structure and observed at 1082 cm^{-1} C–O stretching of acetyl groups [33,34]. The existence of small amounts of oxygen-containing groups on the GNP is associated with the O element included in the composition of PVA.

The stretching frequency corresponding to the C– C stretching was found at around 820 cm^{-1} [33]. The wavenumber of 1260 cm^{-1} sharply observed in the 1- deposited layer might be due to the presence of O–H deformation of PVA, which is not observed during the 2nd and 3rd depositions [35]. This peak weakened with the increase in the number of deposited layers. Depending on the number of deposition, this is associated with surface coverage, reduced incoming signal, changes in intermolecular interactions, and changes in molecular configuration.

The absorption peak corresponding to 1327 cm^{-1} is attributed to the O-C=O asymmetric stretching vibrations [26].

3.4. Raman spectroscopy

Raman spectra of Ag NWs (Fig.6.a), Ag_2S-CdS (Fig.6.b), and GNP (Fig.6.c) are given in Fig. 6.

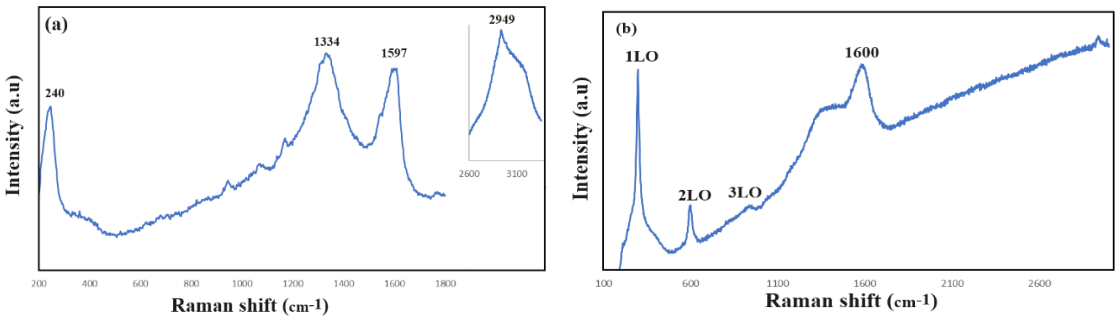

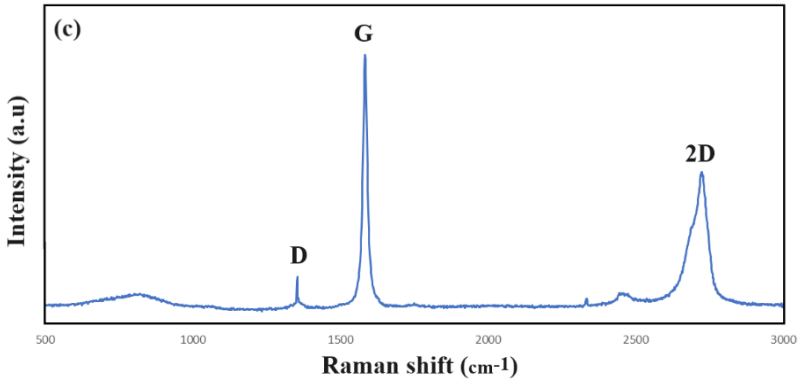

Fig. 6. Raman spectra of a) Ag NWs; b) Ag_2S-CdS and c) GNP.

It consists of vibrational modes at 240.16 cm^{-1}, 1334.20 cm^{-1}, 1597.42 cm^{-1}, and 2949.79 cm^{-1} for Ag NWs (Fig.6.a). The observed peak at 249.21 cm^{-1} corresponds to the Ag–O stretching vibration and Ag–N stretching vibration of Ag with the O residue belonging to the PVP molecule. This demonstrates the interaction of the formed Ag NWs with PVP [36-38].

The peaks observed in the spectrum at 1597.42 cm^{-1} and 1334.20 cm^{-1} correspond to the vibrations of the C=O and C–N polyvinyl pyrrolidone, which corresponds to the G and D bands of amorphous carbon in the PVP polymer matrix [39]. The intensive peak observed at the signal at 2949.79 cm^{-1} is the symmetric stretching vibration of CH_2 in the skeletal chain of PVP [40]. Some shifts of the observed peaks from the characteristic peaks shown in the literature, or differences in intensities are due to the formation of NWs of different sizes and diameters, which can be related to the electronic structure and phonon confinement.

The main observed peaks in the Raman spectrum of Ag_2S-CdS are 300.71 cm^{-1}, 603.35 cm^{-1}, and 948.40 cm^{-1}, respectively first order (1-LO), second order (2-LO) and third order (3-LO) longitudinal-optical (LO) phonon modes of zinc-blende phase CdS, respectively. The characteristic peaks of Ag_2S and Ag_2O observed at about 400 cm^{-1} and 249 cm^{-1} appear as a curve against the background of the intense and broad peak belonging to the 1LO phonon mode belonging to CdS. A very weak peak observed at the end of the spectrum at about 2900 cm^{-1} is a characteristic peak belonging to PVP. Since, in the literature, Ag_2S is also doped with Ni, it exhibits less polarity during the determination of its polarity [41]. In Raman scattering, the loss of the intensity of the LO modes belonging to CdS to its background greater than the intensity of the peaks belonging to Ag_2S and Ag_2O is attributed to the fact that the degree of polarization of CdS is greater than that of them.

At the same time, the peak observed at ~1600 cm^{-1} is considered an important peak related to Ag in Ag–Ag_2 S heterostructures [42].

D peak observed at 1351.77 cm^{-1} was associated with the presence of disorder in the aromatic structure or the edge effect of graphene, G band observed at 1584.32 cm^{-1} is from in-plane C=C bond stretching in graphene (Fig.6.c). The observed peak at 2728.08 cm^{-1} known as the 2D band is related to the thickness [43].

Ag and Ag_2S-CdS NWs were successively deposited on the GNP/PVA composite 1, 2, and 3 times by spin coating method. Raman spectra of the samples obtained from the deposition of NWs 1, 2, and 3 times on the GNP/PVA composite are shown in Fig.7.

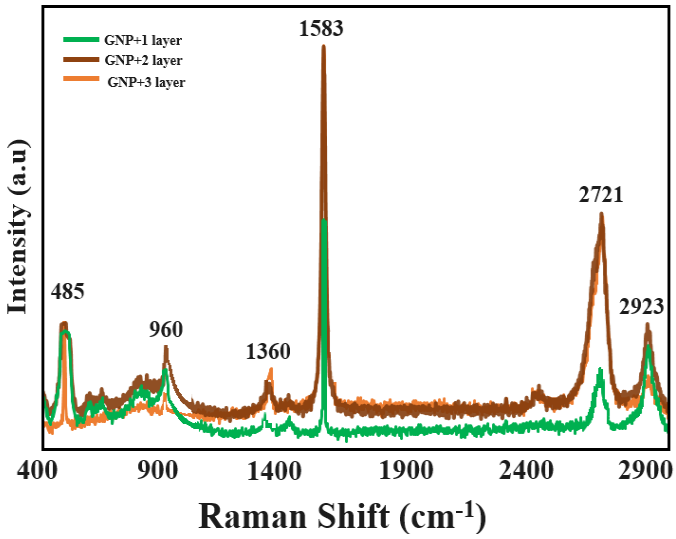

Fig. 7. 1, 2, and 3 times deposition on the GNP/PVA composite.

The sharp peak at 1583.23 cm^{-1} in all three samples is associated with the C-C bond of GNP and is the G band [44]. The fact that this peak is more intense than the other spectra is due to the less surface coverage, where the signals belonging to GNP are more abundant. The peak observed at 2721.12 cm^{-1} is also the characteristic peak belonging to GNP related to the 2D band. The peak observed at a wavenumber of 1360.32 cm^{-1} is related to the D band. For all samples, the other peak which was observed approximately at 2923.47 cm^{-1} range belongs to characteristic peaks of GNP and according to the D-G band [45].

The 485.13 cm^{-1} peak observed in all three samples is a characteristic peak attributed to Ag. It is also clear from other results, that due to CdS covering the surface of Ag_2S, in the spectrum were only observed peaks that related to CdS in the spectrum. In this point of view, the intensity of the peak observed in the interval of 960.22 cm^{-1} is related to the longitudinal optical (3LO) of CdS.

In general, it can be observed from the Raman spectrum that chemical bonds between these hybrid structures were successfully formed, and crystalline structures with different qualities depending on the number of layers were obtained.

3.5. SEM and EDS analysis

SEM images of Ag NWs are given in Fig.8. It is clear from the SEM images that the NWs are formed in a single 1D structure, homogeneous, without agglomeration. Fig. 9 shows SEM images of Ag_2S-CdS nanocomposite materials.

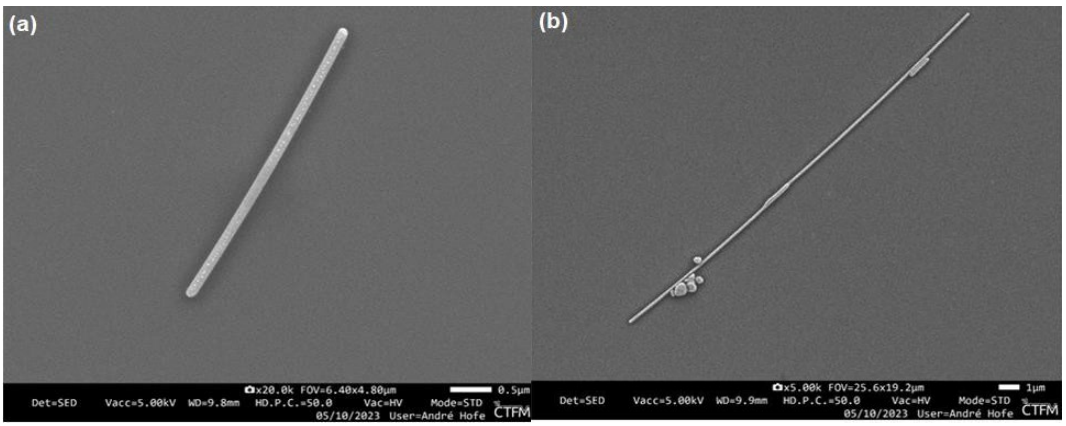

Fig. 8. SEM images of pure Ag NWs.

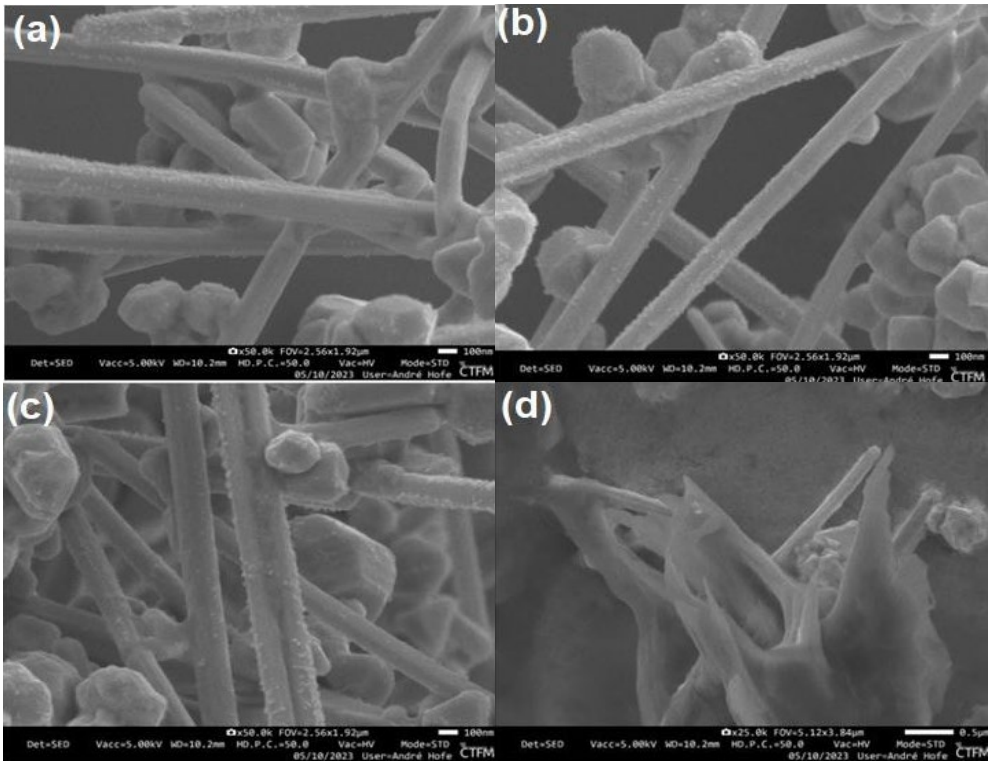

Fig. 9. SEM images of Ag_2S-CdS in different magnification.

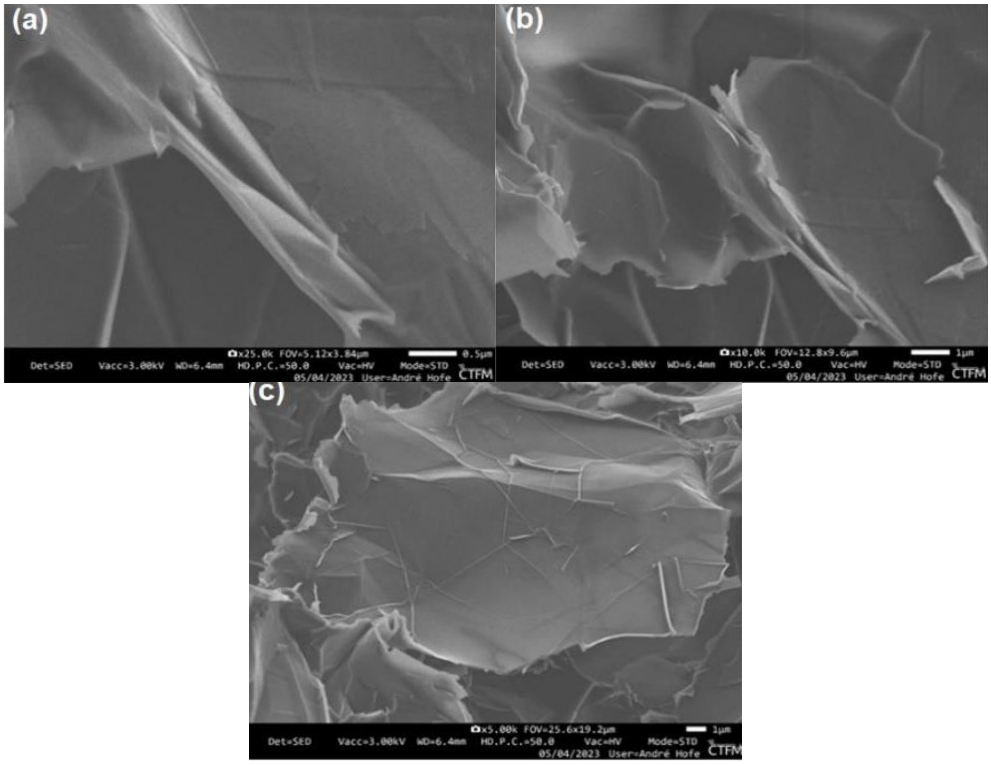

Fig. 10. SEM images of GNP with different magnification.

It is clear from the SEM images that the Ag_2S-CdS nanostructures were formed on the pure Ag NWs and thicker NWs were formed. It is also clear from the SEM images that they cover each other's surface. It is clear from the SEM images that CdS nanostructures are formed in a hexagonal shape and phase on the surface of Ag-Ag_2S NWs.

Fig. 10 shows SEM images of GNP with different magnifications.

From the SEM images, it is clear that the GNP/PVA composite consists of layers. They are wide, leaf-shaped. Fig. 11 shows The SEM images of 1st layer deposited on the glass samples.

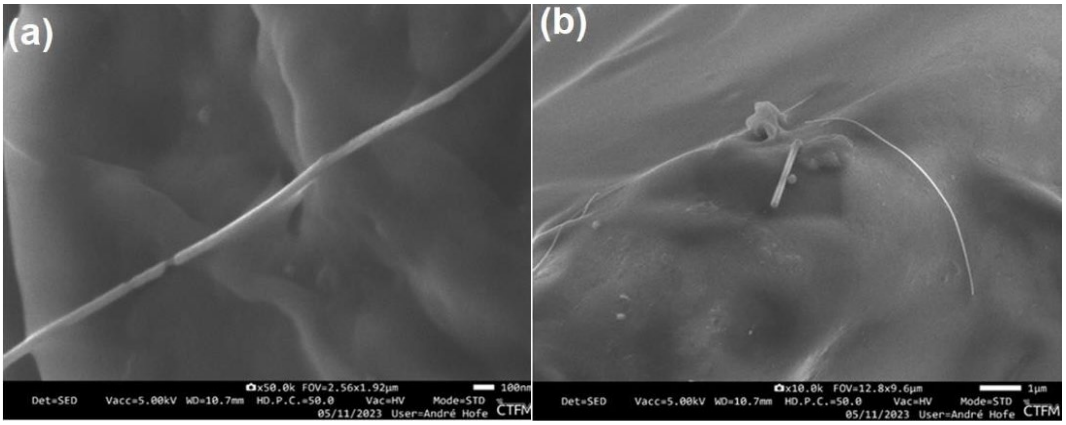

Fig. 11. SEM images of 1 time deposited layer on the glass.

The results clearly show that Ag and Ag_2S-CdS nanostructures are randomly scattered on the glass. Fig. 12 shows The SEM images of the 2nd layer deposited on the glass samples. Here, it is impossible to see the NWs formed between the GNP very clearly. However, with a certain magnification, it was possible to see the formed NWs separately. This means that Ag and Ag_2S-CdS NWs in the nano range were formed between the GNP. Fig. 13 shows The SEM images of the 3rd layer deposited on the glass samples.

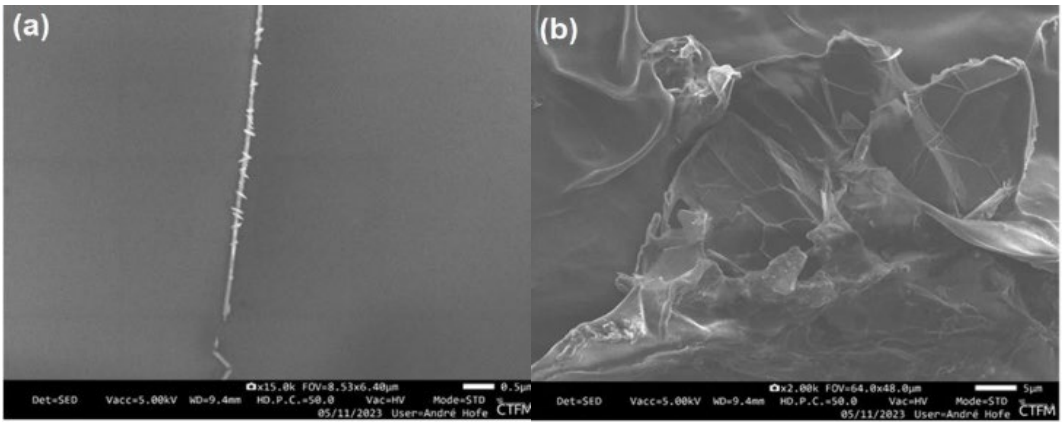

Fig. 12. SEM images of 2 times deposited layer on the glass.

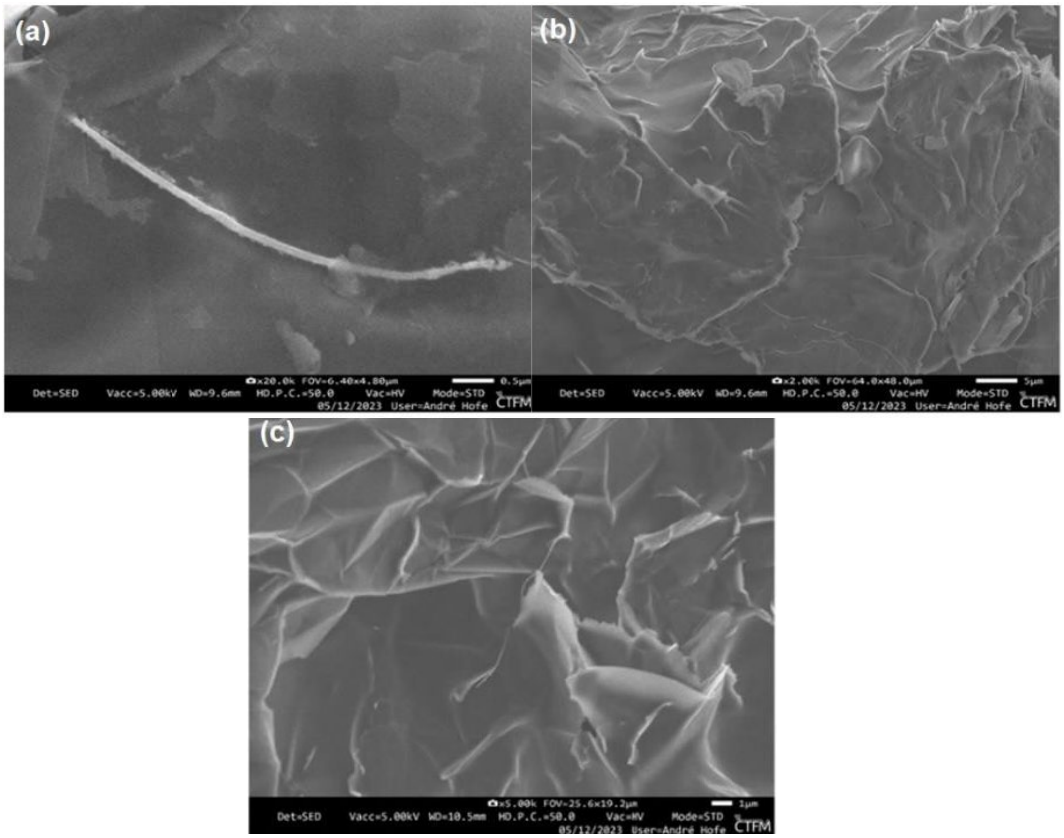

Fig. 13. SEM images of 3 times deposited layer on the glass.

From the SEM images, it is possible to observe the wires formed on the surface of the GNP, as well as, the nanocomposite materials formed around it.

4. Conclusion

Ag_2S-CdS/AgNWs/GNP ternary nanocomposite materials have been synthesized successfully. During the conversion of Ag to Ag_2S, two phases of acanthite Ag_2S and the cubic crystal system of Ag_2O were formed. This result is also reflected in the band gap values of the samples. Thus, the E_g value for Ag is 3.8 eV, for Ag_2S is 2.5, 3.8, 4.6 eV, and the for Ag_2S-CdS compound is 2.5, 3.8, 4.8 eV. Here, the E_g value of Ag_2S as well as the E_g of the Ag_2S-CdS compound had a triple value. A quantity of triple in the E_g value of Ag_2S indicates the formation of Ag, Ag_2S, and Ag_2O. This result was also reflected in XRD. It was determined that the structure of Ag_2S-CdS NWs is a mixed phase. The peaks that belong to silver are monoclinic Ag_2S, and CdS-based peaks belong to the hexagonal phase.

From the Raman spectrum chemical bonds between these hybrid structures were successfully formed, and crystalline structures with different qualities depending on the number of layers were obtained. It was determined that the main peaks in the Raman spectrum of Ag_2S-CdS belong to longitudinal-optical (LO) phonon modes of zinc-blende phase CdS. Here, the characteristic Raman scattering attributed to Ag_2S due to the high polarity of CdS is lost in this background. The results of XRD, SEM, and Raman analyses confirmed that CdS nanostructures were formed in the hexagonal phase. On the surface of GNP/PVA, the peaks belonging to individual NPs appeared at 485.13 cm^{-1} and 960.22 cm^{-1}. From the SEM images, it can be observed that Ag, Ag_2S- CdS is formed in the form of uniform nanowires and layers of GNP.

From the SEM images of Ag and Ag_2S-CdS deposited on GNP, it is possible to observe that their distribution densities increase with the increase of the number of layers on GNP. For the preparation of efficient PV materials, it is possible to increase the diameter of NWs by increasing the concentration of sulfidation, and at the same time, by increasing the number of deposited layers, it is possible to achieve a homogeneous surface.

Acknowledgments

This research was carried out in the framework of COST Action 21148. The authors express their deep gratitude to Dr. André Hofer, the researcher of Chemistry of Thin Film Materials, Friedrich-Alexander-Universität Erlangen-Nürnberg for his invaluable help while doing the analysis.

References

[1] H. Heebo, A. Chiara, M. Paolo, H. Byungil, Coll. and Interface Sci. Comm. 50, 100663 (2022); https://doi.org/10.1016/j.colcom.2022.100663
[2] N. Junaidi, S. Simon, M. Posman, Rev. Chim., 71 (8), 145-156 (2020); https://doi.org/10.37358/Rev
[3] H. Mahboubeh, S. Jan-Henrik, C.B. Juan-Pablo, Energy Environ. Sci.,5, 1377-1407 (2020); https://doi.org/10.1039/C9EE04030G
[4] S.B. Sonal, P. Shashidhar, M.M. Malik, K.P.Piyush, Adv. in Bilayer Graph., 9(3), 70 (2023); https://doi.org/10.3390/c9030070
[5] M. Tahmineh, W.Yousheng, H. Yoon-Bong, Nano Energy, 47, 51-65 (2018); https://doi.org/10.1016/j.nanoen.2018.02.047
[6] J. M. Ramadan, R. G. Mohamed, A. Mujahed, R. Hegazy, Sustainability 12(2), 608 (2020)
[7] Z. Niu, F.Cui, Nano Lett. 18, 5329-5334 (2018); https://doi.org/10.1021/acs.nanolett.8b02479
[8] L.Bo, Y. Shengrong, Nano Lett. 15(10), 6722-6726 (2015); https://doi.org/10.1021/acs.nanolett.5b02582
[9] A. Dabrowska, S.Bellucci, A.Cataldo, F. Micciulla, A. Huczko, Phys. Status Solidi B, 251, 2599-2602 (2014); https://doi.org/10.1002/pssb.201451175
[10] A. Maffucci, F. Micciulla, A. Cataldo, G. Miano, S. Bellucci, Nanotechnology, 27, 095204, (2016); https://doi.org/10.1088/0957-4484/27/9/095204
[11] T.Kuo-Hsiung, Y.Chu-Ti, C.Meng-Yun, L. Yur-Shan, Q.Ning, Sci. Rep., 11(1) 20457 (2021); https://doi.org/10.1038%2Fs41598-021-99976-5
[12] H.Chao, C. Chu, L. Fengling, L. Xinli, W. Guangxin, L. Jiwen, Reviews, 12(1), 20220503 (2023); http://dx.doi.org/10.1515/ntrev-2022-0503
[13] R.B.Srinivasa, K.B. Rajesh, R.R.Varra, R.T. Subba, Chalc. Lett. 8(3), 177-185 (2011); http://dx.doi.org/10.1201/b18247-14
[14] S.I. Sadovnikov, A.I. Gusev, A.A. Rempel, Superlattices and Microstr., 83, 35-47 (2015); https://doi.org/10.1016/j.spmi.2015.03.024
[15] R.Zamiri, A.H.Abbastabari, Chem.Central Journal, 9(28), 1-6 (2015); https://doi.org/10.1186%2Fs13065-015-0099-y
[16] Q.Wang, Y. Wang, Q. Meng, T. Wang, W. Guo, G.Wu, L. You, RSC Advances, 7(5), 2796-2803 (2017); https://doi.org/10.1039/C6RA26458A
[17] P.M. David, T.Amina, R. Billy, N.S. Natalia, Chem. Comm., 53(77), 10715-10718 (2017); https://doi.org/10.1039/C7CC05158A
[18] L.Yiwen, Ch. Jiaji, L. Yizun, L. Peizhao, C. Wanqiang, H. Tingchao, C. Rui, T. Zikang, J. Phys. Chem. C, 121(9) 5208-5214 (2017); http://dx.doi.org/10.1021/acs.jpcc.6b11047
[19] V.Amendola, O. M.Bakr, F. Stellacci, Plasmonics, 5(1), 85-97 (2010); https://doi.org/10.1007/s11468-009-9120-4
[20] S. Yugang, G. Byron, M. Brian, X. Younan, Nano Letters, 2, 165-168 (2002);

https://doi.org/10.1021/nl010093y
[21] S. Perni, V. Hakala, P. Prokopovich, Colloids and Surfaces. A: Physicochemical and Engineering Aspects, 460, 219-224 (2014); https://doi.org/10.1016/j.colsurfa.2013.09.034
[22] P.M. David, T. Amina, R. Billy, N. S.Natalia, Chem. Comm. 53(77), 10715-10718(2017); https://doi.org/10.1039/C7CC05158A
[23] D.A.Rabeea, M.N. Adham, A.P. Osman, A.T. Mahmoud, Y. El Sayed, R. Essam, Optical Materials, 117, 111123 (2021); https://doi.org/10.1016/j.optmat.2021.111123
[24] M. Khademalrasool, M. Khademalrasool, M.Farbod, Journal of Nanostructures, JNS 5, 415-422(2015)
[25] B. Sudarshana, B.S. Bibhuti, K. Avra, M. Nillohit, J. of Indust. and Eng. Chem., 40, 54-61(2016); http://dx.doi.org/10.1016/j.jiec.2016.06.006
[26] H.S. Mahdi, A. Parveen, S. Agrawal, A. Azam, AIP Conference Proceedings, 1832, 2017; http://dx.doi.org/10.1063/1.4980245
[27] A.Lütfiye, Ö. Talat, Theoretical and Vibrational Analysis of Substituted Hydrazones: Valence Force Field, Journal of Institue Of Science and Technology, 38(1), 38-72(2022)
[28] I.Jipa, A. Stoica, M. Stroescu, L.M. Dobre, T. Dobre, S. Jinga, C. Tardei, Chem. Papers, 66(2), 138-143 (2012); https://doi.org/10.2478/s11696-011-0068-4
[29] S.Anitha, M.N. Prasad, N. Jayaram, S. Kumara, B.S. Madhukar, Biosensors and Bioelectronics: X 12, 100255 (2022); https://doi.org/10.1016/j.biosx.2022.100255
[30] X.Peng, Y.Li, G. Zhang, F. Zhang, X. Fan, J. of Nanomat., 11-11(2013); https://doi.org/10.1155/2013/841789
[31] M.Pedram, G.Ismaeil, K. Mohammad, A.Hamed, E.Parvin, Soft Materials, 12:4, 433-444 (2014); http://dx.doi.org/10.1080/1539445X.2014.959598
[32] F.U.Nigiz, Polymer Bulletin, 5, 2405-2422 (2019); http://dx.doi.org/10.1007/s00289-019-02851-7
[33] A.Kharazmi, N. Faraji, R. Hussin, E. Saion, W. Yunus, K. Behzad, J. of Nanotechnology, 6, 529-536(2015); https://doi.org/10.3762/bjnano.6.55
[34] S.Diana, H. Corneliu, V.B. Tăchiță, I. Alina-Mirela, L. Gabriela, A.O. Marius, M.P. Dana, Membranes (Basel)., 13(7), 636 (2023); https://doi.org/10.3390/membranes13070636
[35] A.Shahram, C. Sofia, C. Stefano, Sarco, E.Claudio, M.H.Khaled, P.W. Peter, T.Francesca, V.Alberto, Catalysts, 10, 11 (2020); http://dx.doi.org/10.3390/catal10010011
[36] M. Haibo, F. Jinyang, M. Xiao, W. Can, Z. Xiujian, J Nanopart Res, 14:887, 1-15 (2012); http://dx.doi.org/10.1007/s11051-012-0887-4
[37] J.Chowdhury, M. Ghosh, J. of Coll. and Interface Sci., 277 (1), 121-127 (2004); https://doi.org/10.1016/j.jcis.2004.04.030
[38] P.Mukherjee, M. Roy, B.P. Mandal, Nanotech. 19 (7), 075103 (2008); https://doi.org/10.1088/0957-4484/19/7/075103
[39] G.Yuanning, P. Jiang, P. Jiang, D.F. Liu, J. of Phy. Chem. B, 108(34), 12877-12881(2004); http://dx.doi.org/10.1021/jp037116c
[40] M.Gen-Xiang, C. Yong-Bao, L. Xiao-Guang, H. Zhi-Hua, C. Zhuo-Mei, W. Ya-Zhen, H.Xi-Lian, L. Yuan-Dong, W.Guo-Fu, Y. Jing, J Cardiol,60(6), 495-502 2012; https://doi.org/10.1016/j.jjcc.2012.08.003
[41] H.Poulami, B. Saptasree, D. Diptiman, K.S. Shyamal, American Chemical Societ, 3(12), 17070-17076 (2018); https://doi.org/10.1021%2Facsomega.8b02223
[42] J.Xiong, C. Han, W. Li, Q. Sun, J. Chen, S. Chou, Z. Li, S. Dou, CrystEngComm, 18(6), 930-937, (2016); https://doi.org/10.1039/C5CE02134K
[43] L.Zhang, W.Liu, C. Yue, T. Zhang, P.A. Li, Carbon 61, 105-115 (2013); http://dx.doi.org/10.1016/j.carbon.2013.04.074
[44] A.C. Ferrari, D.M. Basko, Nature Nanotechnol, 8, 235-246. (2013); https://doi.org/10.1038/nnano.2013.46
[45] Pavan, M. V. R., Andrew, R. B. Characterization of Graphene by Raman Spectroscopy, Rice University via OpenStax CNX.